ILD-PHYS-PROC–2026-xxx
19 March 2026

Search for dark photons at future e^+e^- colliders

Mikael Berggren *

On behalf of the ILD concept group.

* *Deutsches Elektronen-Synchrotron DESY,*
Notkestr. 85, 22607 Hamburg, Germany

Abstract

In a class of theories, dark matter is explained by postulating the existence of a 'dark sector', which interacts gravitationally with ordinary matter. If this dark sector contains a U(1) symmetry, and a corresponding 'dark' photon (A_D) , it is natural to expect that this particle kineticly mix with the ordinary photon, and hence become a 'portal' through which the dark sector can be studied. The strength of the mixing is given by a mixing parameter (ε). This same parameter governs both the production and the decay of the A_D back to SM particles, and for values of ε not already excluded, the signal would be a quite small, and quite narrow resonance: If ε is large enough to yield a detectable signal, its decay width will be smaller than the detector resolution, but so large that the decay back to SM particles is prompt. For masses of the dark photon above the reach of Belle II, future high energy e^+e^- colliders are ideal for searches for such a signal, due to the low and well-known backgrounds, and the excellent momentum resolution and equally excellent track-finding efficiency of the detectors at such colliders. This contribution will discuss a study investigating the dependency of the limit on the mixing parameter and the mass of the A_D using the $A_D \to \mu^+\mu^-$ decay mode in the presence of standard model background, using fully simulated signal and background events in the ILD detector at the ILC Higgs factory. In addition, a more general discussion about the capabilities expected for generic detectors at e^+e^- colliders operating at other energies will be given.

Contributed to the Linear Collider Workshop (LCWS2025)
20-24 October 2025
Valencia, Spain

1 Introduction

Numerous cosmological and astronomical observations clearly confirm the existence of dark matter (DM), which accounts for 85% of the matter in the universe. Weakly Interacting Massive Particles (WIMPs) continue to be the focus of observational efforts, but all such attempts have failed so far. This has led to another hypothesis that dark matter exists in a *dark, hidden sector* in which its interaction with the visible sector is extremely weak.

Feebly interacting particles (FIPs) are one type of such model. In these models, dark matter resides in the "dark sector", which is neutral with respect to the Standard Model (SM) and interacts with the visible sector only via gravity. However, it is thought that part of the dark sector interacts with the visible sector, albeit in a very weak form. Therefore, in these models, the reason BSMs have not yet been observed is not due to a lack of energy, but rather a lack of precision - whether in terms of luminosity, sensitivity, background levels, or detector performance.

The mechanism that acts as a "window" into this dark region is known as the portal. There are many types of portals, and they are generally classified according to their composition into Higgs portals, fermion portals, pseudo-scalar portals and vector portals. These correspond to cases where the Higgs particle, a sterile neutrino, an axion-like particle (an ALPS), or a dark photon act as the mediator, respectively. Here we will examine the latter.

2 The Vector Portal - Dark Photons, A_D

Assume that there is a dark sector with a dark U(1) symmetry. The relevant part of the Lagrangian is [2]:

$$\mathscr{L}_{gauge} = -\frac{1}{4}\hat{B}_{\mu\nu}\hat{B}^{\mu\nu} - \frac{1}{4}\hat{Z}_{D\mu\nu}\hat{Z}_D^{\mu\nu} + \frac{1}{2}\frac{\varepsilon}{\cos\theta_W}\hat{Z}_{D\mu\nu}\hat{B}^{\mu\nu} + \frac{1}{2}m_{D,0}^2\hat{Z}_D^{\mu}\hat{Z}_{D\mu}$$

$\hat{B}$ is the ordinary U(1) field-strength tensor, and $\hat{Z}_D$ that of the dark U(1). The Dark Photon (the A_D) might mix with the photon by *kinetic mixing*- the $\hat{Z}_D\hat{B}$ term - so that $e^+e^- \to A_D \to f\bar{f}$ is possible.

The free mixing parameter, ε, must be small; otherwise, this process would have been observed by now. Few events will occur, but their decay will form a very narrow peak, or even a displaced vertex.

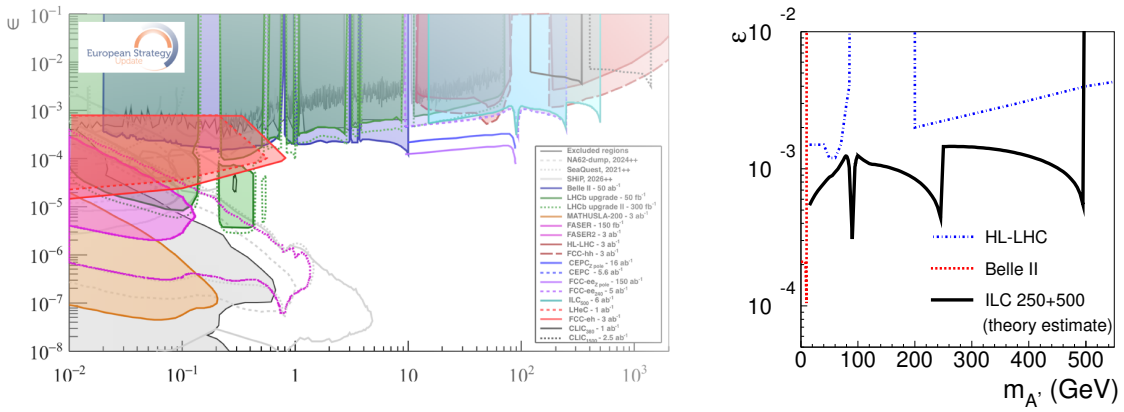

(a) (b)

Figure 1: Expected Dark photon limits from 2019 EPPSU briefing-book [1]. (a) Original figure, with all experiments considered and on a logarithmic mass-scale; (b) the same on a linear mass scale (up to the reach of the higgs factories), only showing the relevant experiments on this scale (Belle II, ILC 250 and HL-LHC).

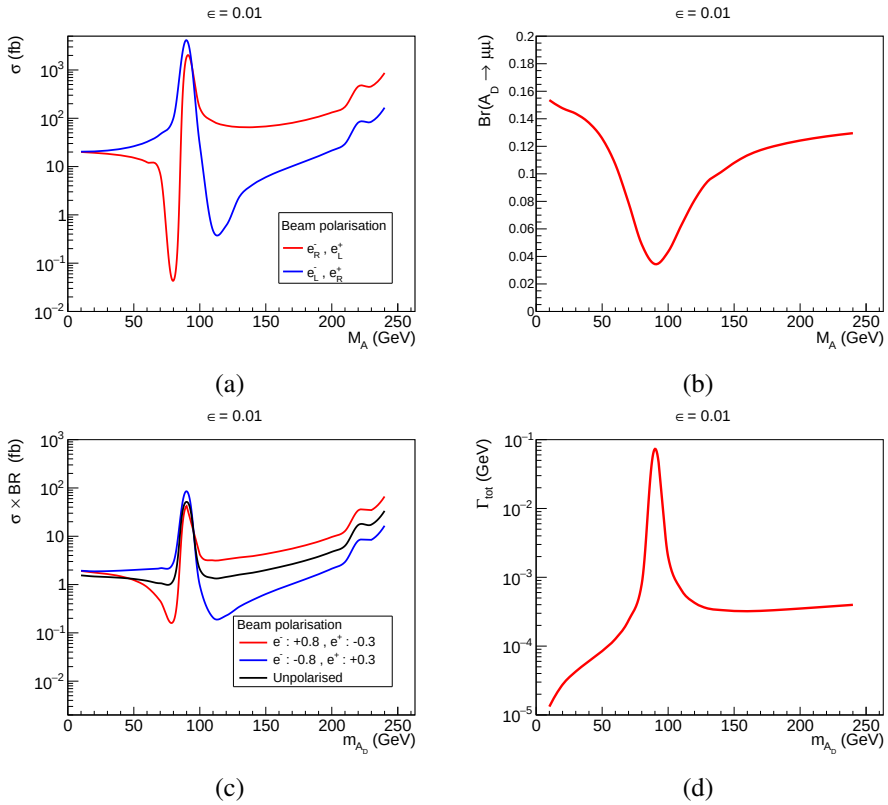

Figure 2: (a): Cross-section of $e^+e^- \to \gamma_{ISR} A_D \to \mu^+\mu^-\gamma_{ISR}$, for the beam polarisations given in the legend; (b) Branching ratio of $A_D \to \mu^+\mu^-$ (c): Cross-section times branching ratio of $e^+e^- \to \gamma_{ISR} A_D \to \mu^+\mu^-\gamma_{ISR}$, for the beam polarisations given in the legend; (d) Total width of A_D.

One must not forget that the dark photon itself is not the DM particle, as it is unstable; for this, another, stable particle is also required in the dark sector.

The current projections for Dark Photon limits from the 2019 update to the "European Strategy for Particle Physics" [1] are shown in Figure 1(a), and on the linear mass scale, they are shown in Figure 1(b). In the mass range up to ~ 1 GeV, dark photons have long lifetimes and are likely to be detected more effectively in beam-dump experiments. At higher energies, colliding particle accelerators are required. Up to 10 GeV, the B-factories are the most powerful tool due to their extremely high luminosity. At higher energies, e^+e^- up to the maximum energy provide the best sensitivity, and beyond that, hadron colliders show some effectiveness, but only if the coupling constant is quite high. It should be noted that the curves for the ILC (and CepC, FCCee) are highly simplified theoretical estimates [3] and, as we shall see later, these are clearly too optimistic.

3 Dark Photons at Higgs factories and beyond

The proposed linear collider facilities acting as Higgs factories are the International Linear Collider (ILC) [4], the proposed Linear Collider Facility (LCF) [5], the Cool Copper Collider (C3) [6], and the Compact Linear Collider (CLIC) [7]. In addition to operating at the optimal energy for Higgs boson research, these facilities are expected to benefit from energy upgrades that will enable them to reach TeV-scale energies. Circular colliders - the Circular Electron-Positron Collider (CEPC) [8] and the Future Circular Collider (FCCee) [9] focus more on low energies (although it is possible to increase

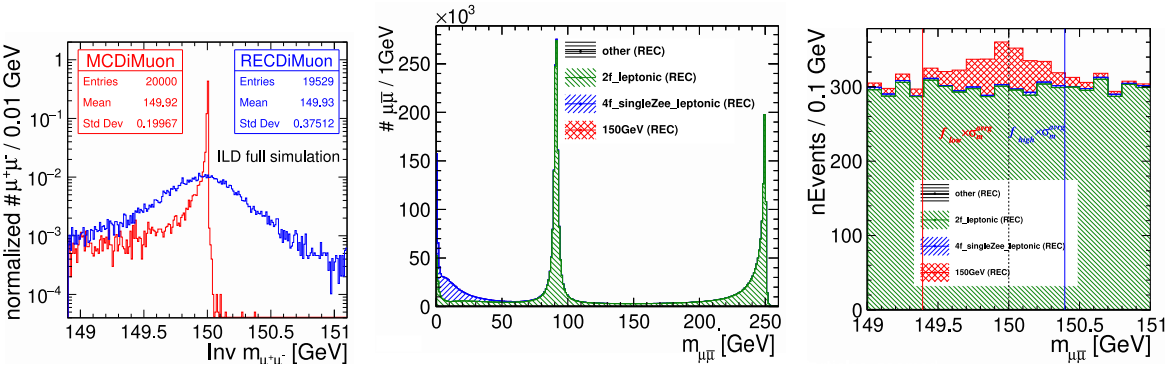

(a) (b) (c)

Figure 3: Di-muon mass distributions for m_{A_D} = 150 GeV from full simulation of ILD: (a): Generated di-muon mass distribution (red), and reconstructed (blue), for a dark photn with mass 150 GeV. (b): as (a), but also including all backgrounds; (c) is the same as (b) zoomed into the signal region.

the energy to 365 GeV). In particular, very high luminosity can be achieved when operating at the Z-pole. Although these facilities, at their Higgs factory stage, only reach marginally higher than what did LEPII, a significant improvement in detection limits for the search for A_D is expected: They will have a luminosity at least 1,000 times higher and - in the case of linear machines - are characterised by trigger-free operation and by having polarised beams. Added to this is the benefit of 40 years' experience in detector development, and indeed, numerous detector concepts have been proposed. In this work, based on [10], we have investigated the capabilities of one of these namely the International Large Detector concept (ILD) [11] at the ILC operating at 250 GeV.

The signal process for A_D production in e^+e^- collisions is as follows: $e^+e^- \to \gamma_{ISR} A_D \to \mu^+\mu^-\gamma_{ISR}$, where the energy of the ISR is such that the recoil mass for the ISR is m_{A_D}. To study this process, we generated events in accordance with the model presented in [2]. We used the Unified Feynrules output file describing the model, provided by the authors, as input data for the event generator `Whizard` (ver. 3.0) [12]. We see that both the production cross-section (σ) and the decay width (Γ) are proportional to ε^2. As a rough estimate, it seems likely that in every Higgs factory, $\sigma > \mathcal{O}$ (1 fb) can be reached. As for the value of ε^2 that yields such an order of magnitude for the cross-section times branching ratio (see Figure 2(c)), it turns out that Γ varies, depending on the mass of the dark photon, from $\mathcal{O}$(10 keV) to $\mathcal{O}$(10 MeV). (See Figure 2(d)). This implies that the decay occurs instantaneously with a $c\tau < 1$ nm, and that the width of the observed peak is determined not by the natural width but by the resolution of the detector (see Figure 3(a)).

4 Dark Photons in a real detector

The generated events were then processed through ILD full simulation (`ddsim` [13]), based entirely on `Geant4`, and full ILD reconstruction chain (`Marlin` [14]). In the analysis, the entire fully simulated SM background was taken into account [15][1]. The subsequent procedure involved only selecting events containing two muons and, possibly, an isolated photon, but nothing else. In the sample of selected two-muon events, we search for an arbitrarily small peak within the $m_{\mu\mu}$ distribution. Its width is determined by the detector resolution rather than the intrinsic width. Figure 3(b) shows the total mass spectrum,

[1] $e^+e^- \to \mu^+\mu^- + ISR$ not only contributes to the background, but also t-channel processes involving undetected beam-remnant electrons, as well as those mistaken for ISR photons. These were also taken into account.

including all backgrounds. Figure 3(c) is an enlarged view of the signal region, corresponding in this case to a dark photon with a mass of 150 GeV.

Figure 4(a) shows the efficiency to detect the two muons as a function of the dark photon mass. The detection efficiency is only about 25% for m_{A_D} = 10 GeV, but approaches 100% when m_{A_D} is equal to or greater than 100 GeV. This can be understood from Figure 4(b) which shows the angular distribution of the two muons for four different dark photon masses.The green square marks the detection area of the track detectors and, as can be seen, a significant proportion of events are lost, especially for the smallest masses, for the simple reason that at least one of the muons lies at angles smaller than the acceptance of the track detectors.

One can make a simple estimate of the mass resolution by assuming that the direction of the ISR lies along the beam axis. Under the further assumption that $\sigma(1/p_T)$ is independent of p, and since $M^2 = p_1 p_2(1-\cos\theta_{12})$, error propagation yields that $\sigma_m \propto m^2$. This is the assumption used in [3] to obtain the exclusion limits presented in the briefing book (Figure 1), which also assumes that the background consists exclusively of $e^+e^- \to \mu^+\mu^- + \gamma_{ISR}$. However, due to multiple scattering, for $p \lesssim 100$ GeV, $\sigma(1/p_T)$ is *not* constant, and one observes a strong dependence on θ when the muon is detected in the forward region rather than in the barrel region (Figure 5(a)). Figure 5(b) shows that most produce muons have momenta where multiple scattering dominates the momentum resolution, and Figure 4(b) shows that most of the muons are at lower angles (below the barrel region of the tracker). Furthermore, the ISR is not always at a zero angle to the beam: if this were the case, the muons would lie exactly on the curves with the greatest number of entries in Figure 4(b). In reality, none of the assumptions regarding mass resolution - the red curve in Figure 6(a) - used for the EPPSU curve are valid. The correct and complete result of the full simulation is the blue curve. Due to the considerable fluctuations in momentum resolution as a function of momentum and polar angle as well as the angle of the ISR photon , the resolution will vary considerably from one event to another. An event-by-event simulation

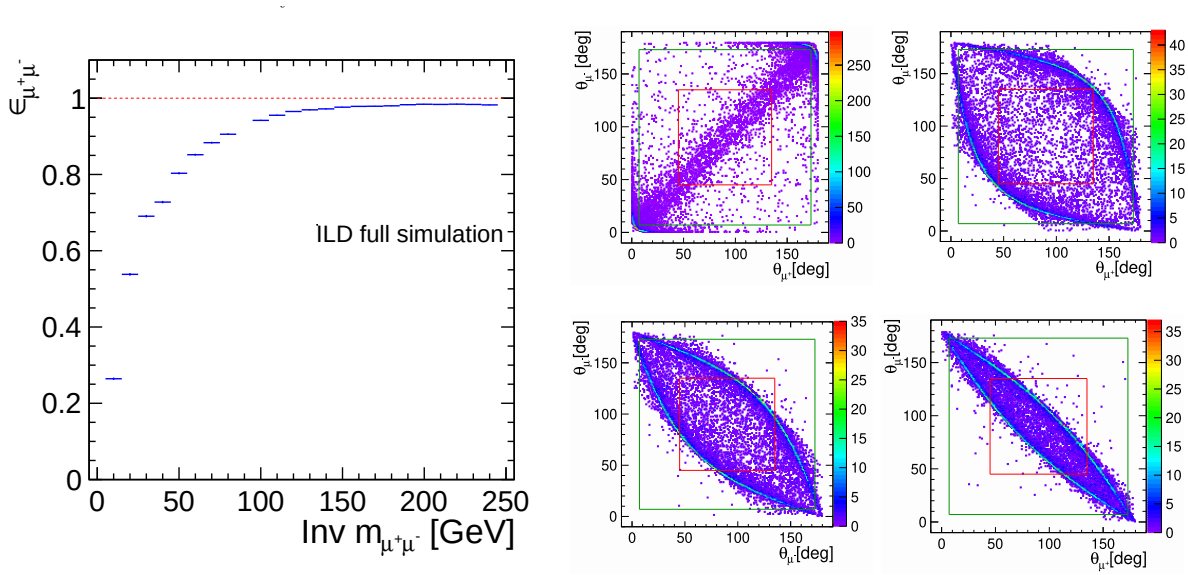

(a) (b)

Figure 4: (a) The efficiency to find both muons from the decay of a A_D vs. m_{A_D}; (b) The polar angle of the μ^- versus that of the μ^+ of the generated $e^+e^- \to \gamma_{ISR} A_D \to \mu^+\mu^-\gamma_{ISR}$ events, for m_{A_D} = 10, 100, 150 and 200 GeV (clock-wise, from upper-left). The green square indicates the acceptance of the tracking system of ILD, and the red one indicates the coverage of the barrel tracking system;

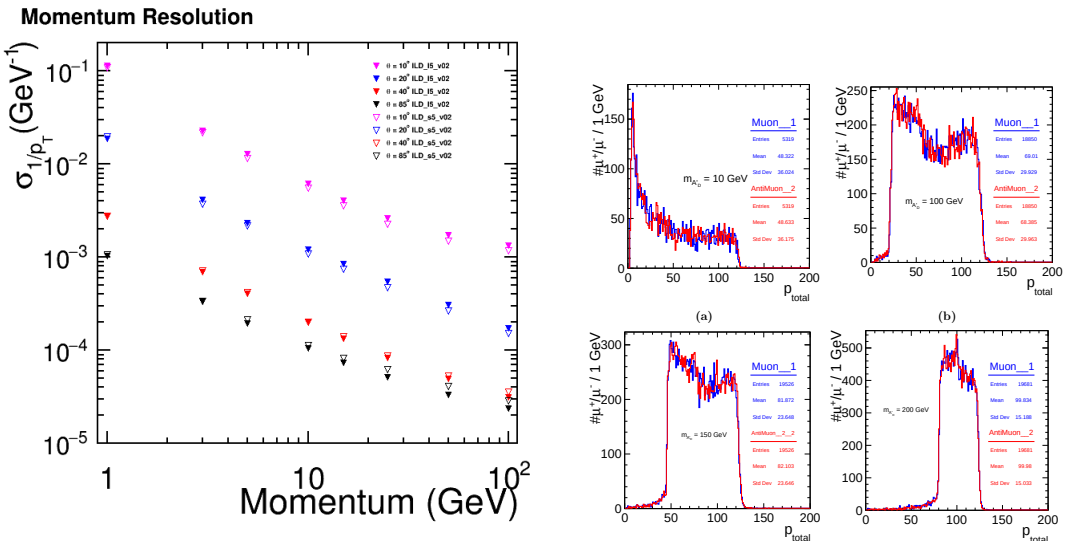

(a) (b)

Figure 5: (a): Momentum resolution for charged particles in ILD from full detector simulation; (b): Momentum of muons from A_D decays at several values of m_{A_D}.

is therefore essential.

Note that since the uncertainty of the mass is known, event-by-event, the search can be optimised for sensitivity by finding the factors f_{low} and f_{high} in an event-specific search window from $f_{low}\sigma_m$ to $f_{high}\sigma_m$ around the probed mass that yields the highest sensitvity. These factors are different above and below the tested mass, because of final state radiation off the muons, which tends to produce a tail in the observed

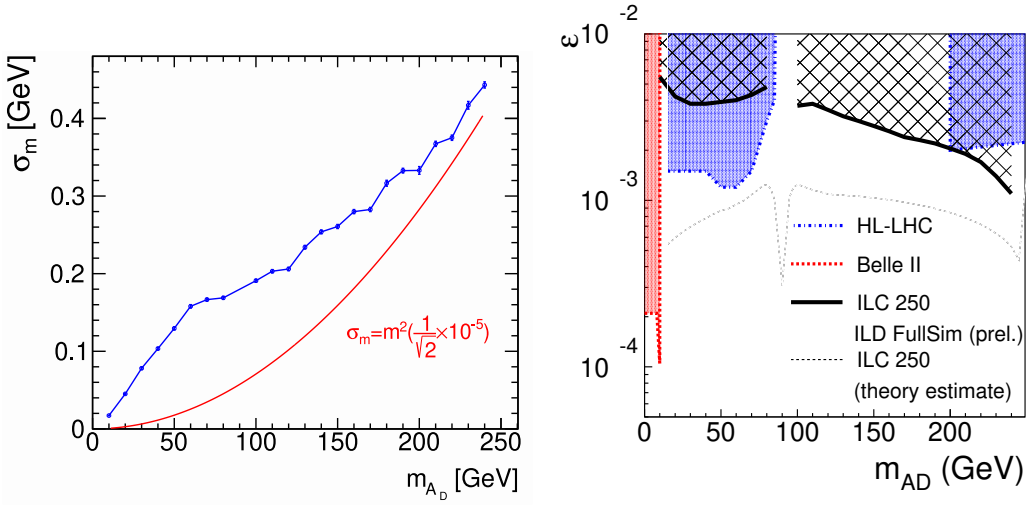

Figure 6: (a): The di-muon mass resolution versus m_{A_D}. The blue curve is the full simulation results, the red one is the simplified theory level one used in [1, 3]; (b): The exclusion reach of ILC 250 obtained from this full simulation study of ILD, and the expectations of Belle II and HL-LHC (from [1])

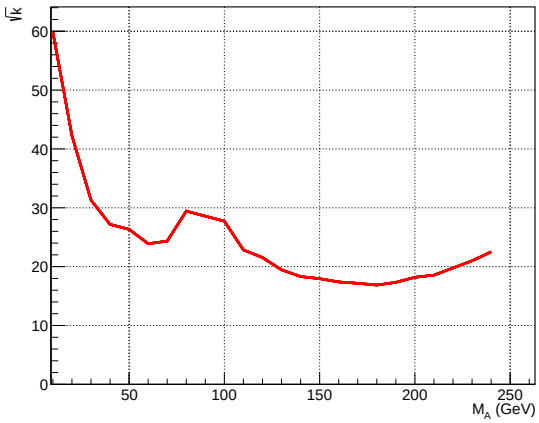

Figure 7: The factor $\sqrt{k}$ relating the signal and background levels at the 95% CL bound.

mass distribution towards lower masses.

5 Expected exclusions at ILC250 and recasts to LCF250, LCF550 and LCF1000

The result obtained in [10] with full simulation is shown in Figure 6(b). Compared with the simple, theory level, estimate (Fig 1(b)), one sees that at the highest mass, the correct limit is a factor two higher than the naïve estimate, a factor four at 100 GeV. This is due to estimating the momentum uncertainty correctly. Below M_Z, the difference is larger, and in fact the HL-LHC limits are expected to be stronger. Here, the reason is both due to using a correct error-estimate, but also due to the much larger background from non-$Z \to \mu\mu$ processes.

The result of the full simulation analyis at ILC250 can be re-cast to quite acurately estimate the reach at the Linear Collider Facility operating at 250, 550 or 1000 GeV. For LCF250 it is quite straight-forward: one only need to scale to the higher luminousity expected at LCF250 w.r.t. ILC250. One should keep in mind that $\sigma \propto \varepsilon^2$, so twice the luminosity limit will improve with the inverse of the *fourth* root of the luminosity increase, not the square root. Hence, the increase in luminosity from ILC250 to LCF250, i.e. from 2 to 3 ab^{-1} only reduces the limit in ε by $1/\sqrt[4]{1.5}$=0.90. In addition, Likelihood-weighting of the different polarisation samples can be applied - this was not done in [10]. However, since signal and the background from $e^+e^- \to \mu^+\mu^-$ has the same polarisation dependence, Likelihood-weighting only helps a lower masses, where other backgrounds, with different polarisation dependence, dominate.

At the higher centre-of-mass energies at LCF550 and LCF1000, several aspects enter. The luminousties are different, the cross-section for the signal will be different, and higher dark photon masses can be probed. To take this into account, it is suffcient to recalculate the cross-section at different, higher masses and centre-of-mass energies with the same tools (WHIZARD and the UFO model) as were used for the ILC250 analysis. The branching-ratio to muons change with the dark photon mass. However, lower E_{CM} will always give better limits up to the kinematic limit, so for LCF550 we can start scanning $M_A >$ at 250 GeV, for LCF1000 at 550 GeV. For those masses, the branching ratio to muon-pairs is constant (see Figure 2(b)), as is the efficiency to find the muon-pairs (see Figure 4(a)). In addition, the background is found to be entirely composted by $e^+e^- \to \mu^+\mu^-$ at these higher masses. The remaining question is what the background level will be at constant signal efficiency. This can be evaluated as follows: For dark photons to muon-pairs, the signal cross-section is proportional to the SM cross-section

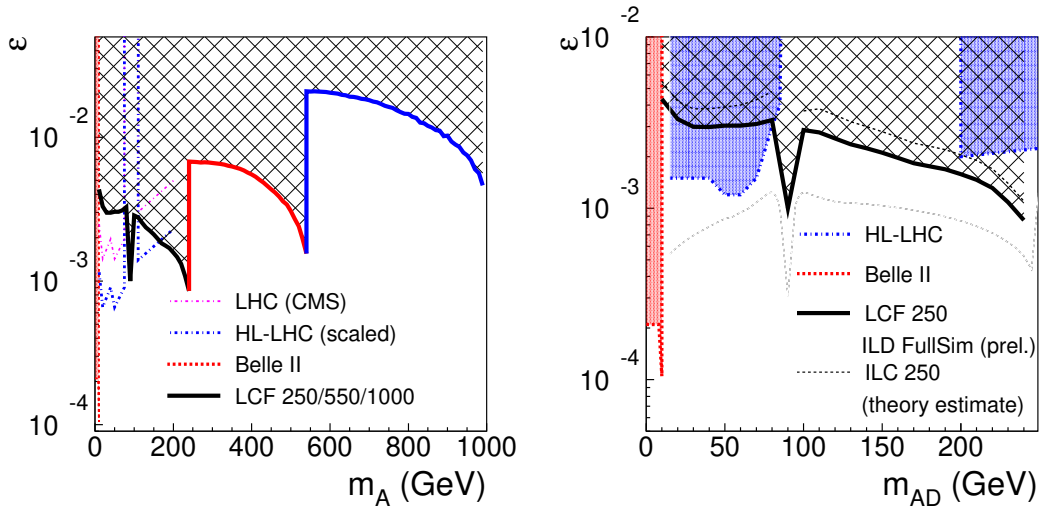

(a) (b)

Figure 8: (a): Expected limits at LCF250, LCF550 and LCF1000, after doing the recast explained in the text. The current limits from CMS and Belle II, as well as a scaling of the CMS limits to HL-LHC are also shown; (b): a zoom to the masses up to 250 GeV, also showing the ILC250 full-sime result, used as an input to the LCF recasts.

for $e^+e^- \to \mu^+\mu^-$. Therefore, for $M_A > 250$ GeV (actually for $M_A \gtrsim 100$ GeV already) , signal and background scale the same way. To keep the same signal efficiency, the search window should scale with the mass-resolution (σ_m). At all masses, this will be a quite narrow window, so that he background will be flat. Therefore, one expects that the background will scale with the mass-resolution, and this mass-resolution can be calculated [2].

If one assumes that B scales with S, i.e. that $B = k\sigma_m S$, one can determine what the factor k is at limiting value of ε by noting that at the limit $S_{lim}/\sqrt{B} = 2$. By putting in the numerical values found in the the Full-sim analysis ot ILC250 one can solve for $\sqrt{k}$: $\sqrt{k} = \frac{1}{2}\frac{1}{\sqrt{\sigma_m}}\frac{1}{\sqrt{\sigma\eta Br\mathscr{L}\varepsilon_{lim}^2}}$ The result is shown in Figure 7, and it can be concluded that $\sqrt{k} \approx$ constant = 20 once $M_A > 100$ GeV. This argument can then be inverted to calculate ε'_{lim} at another point, with different (but known) $\sigma_m, \sigma, \mathscr{L}$ and $\sqrt{k} = 20$: to yield $\varepsilon'_{lim} = 2\sqrt{k}\sqrt{\sigma'_m}\frac{1}{\sqrt{\sigma'\eta Br\mathscr{L}'}}$. The resulting exclusion-reach for all LCF options is given in Figure 8(a), and in Figure 8(b) the case of LCF250 is shown, compared to the ILC250 curves both for the full simulation analysys, and the theory estimate.

6 Conclusion and outlook

Even in the simplest topologies - or perhaps precisely in those - a full simulation is required to obtain a realistic result. For in these cases, accuracy is the most important factor. However, even if the correctly evaluated range is significantly lower than the theoretical estimate, the e^+e^- colliders allow the investigation of weaker dark photon couplings than at the HL-LHC, at least for masses greater than M_Z.

It would be interesting to have a serious evaluation of the prospects for FCCee, up to its limited maximum reach of 365 GeV. Since full detector simulation, with full SM background is lacking for FCCee, firm conclusions will have to wait. At lower masses, the huge luminosity at FCCee, in particular

[2] This calculation is not trivial, and will be the topic of a future publication.

at the Z-pole, will certainly out-perform LCF, and might even compete with Belle II. However, it is probable the results at FCCee at the higher masses will be not better than LCF: FCCee will collect more luminosity, but the detectors will necessarily be less performant, since the FCCee conditions require lower detector B-field, and more material due to the need of cooling. Hence, the mass-resolution, crucial for this analysis, will be worse.

This is an ongoing study. There is still room for improvement in the analysis. We have considered only the muon channel. This is because the muon channel is expected to exhibit the best mass resolution. It would also be possible to include $A_D \to e^+e^-$; however, to achieve sufficient mass resolution, it would be necessary to develop a method to compensate for bremsstrahlung.

Furthermore, by utilising the properties of the detected ISR, it should be possible to reduce background noise when m_{A_D} is small. To make the most of the insights gained regarding errors at the event level, one could also consider an approach based on the unbinned maximum likelihood method.

Finally, it is clear that the sensitivity is greatest when the collider operates at or near the dark photon mass. One might therefore consider devoting part of the operating time to a scan of E_{CMS}, provided that this does not pose any difficulties from the point of view of the facility's operation. Among the proposed Higgs factories, only the LCF, ILC and C3 offers this possibility.

7 Acknowledgements

We would like to thank the LCC generator working group and the ILD software working group for providing the simulation and reconstruction tools and producing the Monte Carlo samples used in this study. This work has benefited from computing services provided by the ILC Virtual Organisation, supported by the national resource providers of the EGI Federation and the Open Science GRID.

References

[1] Richard Keith Ellis et al. "Physics Briefing Book: Input for the European Strategy for Particle Physics Update 2020". In: (Oct. 2019). arXiv: 1910.11775 [hep-ex].

[2] David Curtin et al. "Illuminating Dark Photons with High-Energy Colliders". In: *JHEP* 02 (2015), p. 157. arXiv: 1412.0018 [hep-ph].

[3] Marek Karliner et al. "Radiative return capabilities of a high-energy, high-luminosity e^+e^- collider". In: *Phys. Rev. D* 92.3 (2015), p. 035010. arXiv: 1503.07209 [hep-ph].

[4] "The International Linear Collider Technical Design Report - Volume 1: Executive Summary". In: (June 2013). Ed. by Ties Behnke et al. arXiv: 1306.6327 [physics.acc-ph].

[5] C. Balazs et al. "The Linear Collider Facility (LCF) at CERN". In: (Mar. 2025). arXiv: 2503.24049 [hep-ex].

[6] Caterina Vernieri et al. "Strategy for Understanding the Higgs Physics: The Cool Copper Collider". In: *JINST* 18.07 (2023), P07053. arXiv: 2203.07646 [hep-ex].

[7] O. Brunner et al. "The CLIC project". In: (Mar. 2022). arXiv: 2203.09186 [physics.acc-ph].

[8] J. Gao. "Snowmass2021 White Paper AF3-CEPC". In: (Mar. 2022). arXiv: 2203.09451 [physics.acc-ph]

[9] G. Bernardi et al. "The Future Circular Collider: a Summary for the US 2021 Snowmass Process". In: (Mar. 2022). arXiv: 2203.06520 [hep-ex].

[10] Sepideh Hosseini-Senvan. "Dark Photon Searches at Future e^+e^- Colliders". MA thesis. University of Hamburg, 2024.

[11] Halina Abramowicz et al. "International Large Detector: Interim Design Report". In: (Mar. 2020). arXiv: 2003.01116 [physics.ins-det].

[12] Wolfgang Kilian, Thorsten Ohl and Jurgen Reuter. "WHIZARD: Simulating Multi-Particle Processes at LHC and ILC". In: *Eur. Phys. J. C* 71 (2011), p. 1742. arXiv: 0708.4233 [hep-ph].

[13] M. Petrič et al. "Detector simulations with DD4hep". In: *J. Phys. Conf. Ser.* 898.4 (2017). Ed. by Richard Mount and Craig Tull, p. 042015.

[14] F. Gäde. "Marlin and LCCD: Software tools for the ILC". In: *Nucl. Instrum. Meth. A* 559 (2006). Ed. by J. Blumlein et al., pp. 177–180.

[15] Mikael Berggren. "Generating the full SM at linear colliders". In: *PoS* ICHEP2020 (2021), p. 903. arXiv: 2105.04049 [hep-ex].